Mon. Not. R. astr. Soc. (1974) **169**, 35–57.

THE GROWTH AND DECAY OF SUNSPOTS

F. Meyer, H. U. Schmidt, N. O. Weiss and P. R. Wilson

(Received 1974 June 12)

SUMMARY

The evolution of a sunspot is related to supergranular convection. Magnetic flux is concentrated by converging supergranular flow to form the sunspot. Equilibrium requires a magnetic field strong enough to inhibit convection in the photosphere but small scale convection is still possible at depths greater than 2000 km below the spot. The region surrounding this flux rope is imperfectly cooled. As a result the direction of flow in adjacent supergranules may be reversed. If the flux rope is inclined or split it may be broken up and the spot will decay rapidly; if it is predominantly vertical the reversed flow forms an annular cell (corresponding to the moat) about the spot, which is preserved through a phase of slow decay. The strong field prevents large scale convection in this cell from penetrating into the flux rope beneath the spot but small flux tubes diffuse outwards at a rate which is determined by the modified small scale convection. They are then torn away from the penumbra and carried across the moat, appearing as moving magnetic features in the photosphere. A simple model of this decay process explains the observed linear decay of flux with time and is supported by some numerical experiments.

1. INTRODUCTION

Cowling (1946) concluded that the growth and decay of the magnetic field in a sunspot ' cannot be due solely to electro-magnetic effects in the absence of convection but must be due, at least in part, to mass motion '. Recent observations have revealed many fascinating details of the convection pattern around sunspots and the associated transport of magnetic flux. The aim of this paper is to construct a coherent description of the formation and destruction of sunspots that is consistent both with these observations and with our theoretical understanding of the interaction between magnetic fields and convection.

The observations summarized in the next section have recently been reviewed by Vrabec (1974). Sunspots are formed between supergranules, at junctions in the chromospheric network. Many spots disappear rapidly. However, some large spots enter a phase of slow decay: an annular cell develops, centred on the spot and with a systematic outward velocity directed from the penumbra towards the nearest faculae. This flow forms a moat around the spot swept clear of magnetic field except for magnetic features which migrate from the penumbra to the surrounding network. This phase may persist for several months before the spot is finally destroyed. Throughout this period the sunspot area, and hence its flux, decrease at a constant rate.

We shall relate the evolution of a sunspot to subphotospheric convection, with particular emphasis on a model of the slow decay phase which explains the steady decay of magnetic flux. First of all, we describe the equilibrium configuration of a sunspot. Observations are limited to the photosphere: in Section 3 we extrapolate downwards to describe the flux rope underneath a sunspot and relate

it to the ambient convective zone. Energy transport is then discussed in Section 4. The strong magnetic field inhibits convection near the photosphere but at depths greater than 2000 km the increase in opacity owing to ionization reduces the radiative conductivity sufficiently for convection to be possible below the spot. This small scale convection supplies the energy radiated from the umbra and also provides an effective eddy diffusion for magnetic fields.

The development of sunspots has been studied by Parker (1955), Wilson (1968) and Ponomarenko (1970, 1972a, b). The formation of an active region begins with a loop of magnetic flux floating upwards from the deep convective zone. After the flux emerges through the photosphere it is concentrated by supergranular convection to form a sunspot. During this growth phase, the supergranular motion is inward and downward near the spot, leading to convergence of flux. In a fully-developed sunspot the magnetic field fans out immediately below the photosphere, becoming horizontal at the edge of the spot. This spreading penumbral field impedes the removal of heat by supergranules from around the base of the sunspot. The interference with heat transfer reverses the flow around the spot, producing an annular cell with inflow at about 12 000 km depth, a rising motion round the spot column and radial outflow at the surface. This cell preserves the spot through the phase of slow decay. In Section 5 these processes are related to the observations.

A more detailed model of slow decay is given in Section 6. The magnetic flux is contained by two collars, one at the surface (imposed by gas pressure) and one at 12 000 km (due to inflow). Small flux tubes first detached around 6000 km depth can escape from the upper collar, whence the ultimate spot decay. We suppose that lines of force emerging from the Sun through the sunspot constitute a flux rope that is isolated from the annular convection cell that forms the moat, and that the boundary of this flux rope is characterized by a critical magnetic field strength. Between the two collars, small scale convection can occur, allowing flux tubes to diffuse outwards into the surrounding cell. They are then torn away from the penumbra and carried across the moat. This model predicts a constant decay rate for the magnetic flux in the spot. Its main properties are illustrated by a number of simplified numerical experiments which are described in Section 7.

The behaviour of magnetic features as they cross the moat is discussed in Section 8 and related to the field configuration around the sunspot. In conclusion, we suggest some further observations and indicate the problems that remain for theoreticians.

2. THE OBSERVATIONS

It is now possible to observe the Sun continuously at high resolution and so to follow small magnetic features (about 1000 km in diameter) either on magnetograms (Vrabec 1971; Frazier 1972; Harvey & Harvey 1973) or as bright points in CN spectroheliograms (Sheeley 1969, 1971). These magnetic features move into sunspots as they grow and away from them as they decay, with velocities that are consistent with those obtained from Doppler spectroheliograms (Sheeley & Bhatnagar 1971; Sheeley 1972). We shall only summarize these results, which are described in detail by Vrabec (1974).

Magnetic flux first appears at the centre of a supergranule and the emergent flux tube forms an arch filamentary system above the photosphere (Bruzek 1967,

1969; Frazier 1972). The feet of the arch filamentary system migrate to the boundary of the supergranule within a period of 4–5 hr (Frazier 1972). More flux collects in the network and pores appear. Over a few days the pores develop into spots which remain between supergranules but move further apart until they are separated by about 150 000 km. (The diameter of a typical supergranule is 30 000 km.) Vrabec (1971, 1974) has observed small magnetic features of one polarity moving into developing sunspots; these features appear between a sunspot pair and move towards the spot with appropriate polarity. This growth phase lasts for 3–10 days, while the leading spot moves forward in longitude for up to 15 days (Royal Greenwich Observatory 1925; Bumba 1963).

Most spots disappear rapidly within the next few days but some large spots (usually leaders) survive through a long period of slow decay. A remarkable feature of this slow decay phase is that the sunspot area decreases at a constant rate (Royal Greenwich Observatory 1925; Bumba 1963; Bray & Loughhead 1964; Gokhale & Zwaan 1972). Since the field strength scarcely changes, this implies that the rate of decay of magnetic flux remains constant while the flux falls by a factor of 5 from its maximum value (Cowling 1946).

Observations of decaying sunspots show small magnetic features (magnetic knots) moving outwards from the penumbra towards the nearest faculae with velocities of about 1 km s^{-1}. The magnetic flux in an individual knot is about 3.10^{19} mx and the net flux transported by these features across the region surrounding the spot is approximately 10^{19} mx hr^{-1}. This is equal to the constant overall decay rate. However, the moving magnetic features tend to appear in pairs with opposite polarity and the gross flux moving outwards is an order of magnitude more than the flux lost by the sunspot (Harvey & Harvey 1973).

Within the same annular region Sheeley (1972; Sheeley & Bhatnagar 1971) has measured a systematic outflow in the slowly varying component of the photospheric velocity field, with velocities of 0·5–1·0 km s^{-1}. This outward radial flow resembles supergranular motion rather than an extension of the Evershed effect, and Sheeley suggested that it was related to the moving magnetic features. He called this region the moat. It occupies an annular zone about the spot, though irregularities are often present: the moat may be incomplete or sections of network may penetrate across it. All the magnetic flux in the moat is confined to magnetic knots of opposite polarities, moving in the same direction (Vrabec 1974); no other similar feature has been observed. Harvey & Harvey (1973) find that the moat extends for 10 000–20 000 km beyond the edge of the spot, giving a total diameter of up to 60 000 km.

Both supergranulation and the moat must be explained in terms of subphotospheric convection. Sheeley (1972) has described the moat structure by saying that sunspots occur at the centres of supergranules. It seems preferable to distinguish the moat from normal supergranules on account of its size, occurrence and unique relationship to sunspots. Although moat structures are generally observed around slowly decaying spots, observations are not yet adequate to determine whether there is a one to one correspondence. Moreover, the systematic velocities have to be observed near the limb while the magnetic features are best seen near the centre of the disc; so the two phenomena have not yet been simultaneously observed in the same sunspot. We shall nevertheless assume that a slowly decaying sunspot is surrounded by a moat with a systematic outflow and moving magnetic features.

3. THE EQUILIBRIUM OF A SUNSPOT

Before considering time dependent behaviour we must describe a static sunspot and the flux rope that extends beneath it. In particular, we need to understand how energy is transported upwards along this flux rope and what processes limit the energy that emerges from the umbra. In this section we first summarize the features revealed by observations, which are of course limited to a shallow photospheric layer. Then we consider the flux rope beneath the surface and relate its structure to the ambient convective zone. Transport of energy within the flux rope will be discussed in Section 4.

The properties of sunspots have been reviewed by Bray & Loughhead (1964), Zwaan (1968) and, most recently, by Schröter (1971). The concentrated magnetic field inhibits convection and the umbra cools until a dynamic and thermal balance is achieved (Biermann 1941). The properties of an axisymmetric sunspot are then determined by the magnetic flux Φ. For a large spot $\Phi \sim 2 \times 10^{22}$ mx, the penumbral radius is about 20 000 km, the umbral field 3000 G and the umbral temperature 4000 K. Hydrostatic equilibrium requires the field to be almost horizontal at the edge of the spot, so allowing the formation of a penumbra (Simon & Weiss 1970). Near the surface, the external gas pressure p acts as a collar containing the magnetic pressure p_m plus reduced gas pressure within the spot. Although this collar is shallow (the ratio p_m/p drops to 0·025 at a depth $z = 2000$ km), it is clear, empirically, that the configuration is dynamically stable. Sunspots are observed for many days, though the characteristic time for hydromagnetic disturbances is only an hour.

This stability may be related to the Wilson depression: if a flux tube is removed from the umbra thermal and potential energy is needed to heat the plasma and to raise it through about 500 km. A similar argument indicates that sunspots should preferentially be round. For the surface with optical depth unity sinks from its normal photospheric level through about 500 km, in an annular transition zone around the boundary of a spot. The width of this transition zone is determined by the radiative or conductive influx of heat from outside, and the mass of gas within it is proportional to the perimeter of the spot. If the spot is distorted so as to increase the perimeter, work must be done in raising gas into the transition zone. Hence a spot of given area should be stable when its circumference is least, i.e. when it is circular.

The most obvious feature of a sunspot is the uniformity of the umbra as contrasted with the filamentary structure of the penumbra. The inhomogeneous penumbral field (Schröter 1971) is related to the local pattern of convection. Within the umbra, however, the magnetic field appears uniform apart from small scale fluctuations (Harvey 1971; Gokhale & Zwaan 1972). Umbral dots appear sporadically in sunspots; they are small (200 km) regions with photospheric brightness (Beckers & Schröter 1968; Krat, Karpinsky & Pravdjuk 1972). Otherwise the umbral intensity is approximately uniform and any lateral variations could be ascribed to scattered light (Mykland 1973).

The fact that the umbral temperature remains constant throughout the lifetime of a sunspot indicates that the heat transport must be limited by a shallow throttle. Nevertheless, the flux ropes that emerge in sunspots apparently originate in the deep convective zone, where motion is dominated by giant cells (Schmidt 1968). Owing to magnetic buoyancy the field below a long lived sunspot must be nearly

vertical and the flux rope should extend to depths of order 10^5 km. At no stage of a sunspot's evolution is there a significant bright ring to compensate for its reduced intensity of radiation (Wilson 1968). The most direct explanation of this fact is that the reduction in energy transport persists throughout flux tubes which extend sufficiently deep for the energy to be spread over a region whose diameter is comparable with the depth of a convective zone (Danielson 1965). The problem of missing energy cannot be resolved by postulating a large invisible non-radiative flux: this would be enough to supply a large and continuous flare and could scarcely pass undetected through the chromosphere and corona (Piddington 1973). Wilson (1973, 1974a) has suggested that there might be a significant lateral energy flux away from a sunspot if there were a radial outflow from within the flux tube at depths around 5000 km, during the slow decay phase.

We shall assume that the magnetic flux observed in sunspots remains concentrated into flux ropes down to a depth of at least 20 000 km. It is only near the surface that magnetic pressure is significant. The cross-section of the flux tube must decrease rapidly below the photosphere but beneath the collar it will only vary slowly. A crude estimate of the radius of the flux tube can be obtained by supposing that the missing energy corresponds to the normal energy flux across an area equal to that of the flux tube. This yields a typical radius of 12 000 km and an average field of about 3500 G (Weiss 1969).

However, any such estimate of the depth or radius of the flux rope depends on assumptions about the lateral transport of heat. In the absence of a magnetic field, static equilibrium is possible only if all thermodynamic quantities are constant on gravitational equipotentials. Any horizontal density gradient must drive a circulation. Horizontal temperature differences are therefore difficult to maintain. They produce convection and lateral exchange of energy is so efficient that systematic temperature differences are unlikely to penetrate into regions where the scale height is small compared with the horizontal scale of variations in the temperature. This process quickly redistributes any surplus energy flux over a large area. (On a smaller scale, horizontal transport will reduce the temperature differences in supergranules; this may explain the lack of any observable correlation between photospheric temperature and the supergranule network.)

The structure of the flux rope is determined by motion in the convective zone around it. Model convective zones can be computed using mixing length theory, with the mixing length l related to the local pressure or density scale height (Baker & Temesvary 1966); at depths greater than 1000 km below the photosphere the stratification is virtually adiabatic. Table I shows the temperature T, the pressure p, the density ρ and the pressure scale height $H_p = [d \ln p/dz]^{-1}$ as functions of the depth z below the level where the optical depth $\tau = \frac{2}{3}$, for the upper part of a model convective zone calculated with $l = 1{\cdot}5\, H_p$ using the program described by Baker & Temesvary (1966).

Understanding sunspots requires a more detailed picture of the motion. Various alternatives have been discussed by Wilson (1972). We adopt here a model consistent with observations, in which convective energy transport is dominated by three discrete scales of motion, corresponding to granules, supergranules and giant cells (Simon & Weiss 1968; Ponomarenko 1970, 1972a; Weiss 1971). This does not imply that all eddies have the same size at any particular level. Giant cells and supergranules penetrate to the photosphere, where they contribute a negligible flux. Moreover eddies with dimensions corresponding to

TABLE I

Model convective zone

Depth (km)	T (K)	P (dynes cm^{-2})	ρ (g cm^{-3})	H_p (km)
1000	$1{\cdot}5\times10^{4}$	$3{\cdot}3\times10^{6}$	$2{\cdot}9\times10^{-6}$	450
2000	$2{\cdot}0\times10^{4}$	$2{\cdot}0\times10^{7}$	$1{\cdot}1\times10^{-5}$	640
4000	$3{\cdot}0\times10^{4}$	$2{\cdot}1\times10^{8}$	$7{\cdot}2\times10^{-5}$	1100
6000	$4{\cdot}0\times10^{4}$	$9{\cdot}3\times10^{8}$	$2{\cdot}1\times10^{-4}$	1700
8000	$5{\cdot}4\times10^{4}$	$2{\cdot}6\times10^{9}$	$4{\cdot}3\times10^{-4}$	2000
12000	$8{\cdot}4\times10^{4}$	$1{\cdot}0\times10^{10}$	$1{\cdot}0\times10^{-3}$	3700
16000	$1{\cdot}2\times10^{5}$	$2{\cdot}6\times10^{10}$	$1{\cdot}8\times10^{-3}$	5100
20000	$1{\cdot}4\times10^{5}$	$5{\cdot}1\times10^{10}$	$2{\cdot}8\times10^{-3}$	6500
24000	$1{\cdot}8\times10^{5}$	$9{\cdot}1\times10^{10}$	$4{\cdot}2\times10^{-3}$	8000

the local scale height must be generated throughout the zone, though their effect on heat transport is generally small. In particular, there will still be parasitic local motions extending over the region 2000 km $< z <$ 10 000 km, where heat transport is dominated by supergranules with a characteristic scale of 15 000 km. These small scale motions carry a fraction of the flux and also provide a local eddy diffusivity which affects both the heat transport and magnetic fields. The existence of this small scale convection, superimposed on the large scale supergranular flow, is essential for the model to be discussed in Section 6.

Observations confirm that sunspots are related to supergranular convection. A growing spot, at a junction in the network, is surrounded by converging flow probably down to a depth $\gtrsim 10^4$ km. This flow will concentrate magnetic flux and the field near the surface will depend on that produced where the energy of the flow is greatest, at about 10^4 km depth. Below this level the flow must ultimately diverge, producing a swelling or disruption of the flux tube. Around a decaying spot, on the other hand, there is an outflow at the surface, with a corresponding inflow at a level below 10^4 km. This inflow concentrates the flux again.

The magnetic field exerts forces which limit this concentration process. Flux is actively concentrated by the converging flow at depths around 10^4 km until the field is strong enough locally to halt convection. A plausible estimate of this field is obtained by equating the local magnetic energy density to the kinetic energy density of convection. This equipartition field has a value of about 3500 G, which is consistent with the crude estimate obtained above (Weiss 1969).

Thus the magnetic flux emerging from a sunspot is contained by two collars. One, at the surface, is provided by gas pressure. The other, at about 12 000 km depth, is caused by inflow. Moreover, the second collar remains even if the sense of motion round the sunspot is reversed. Transport of energy along the flux tube between these collars will be discussed below.

4. CONVECTION IN THE FLUX ROPE BENEATH A SUNSPOT

Umbral models derived from observations require some non-radiative transport in the photosphere and it is impossible to construct a sunspot model unless some convection is allowed at greater depths (Schlüter & Temesvary 1958; Chitre 1963; Deinzer 1965; Yun 1970). Two questions can be asked: what process governs heat transport near the surface, where the throttle operates, and how

is energy carried in the flux rope below this region? Although no proper theory is available, these problems can be clarified by reference to a specific model.

The theory of convection in a magnetic field is summarized by Cowling (1957). For a Boussinesq fluid, the relevant dimensionless parameters are the Rayleigh number

$$R = \frac{g\alpha\beta d^4}{\kappa\nu} \tag{1}$$

and the Chandrasekhar number

$$Q = \frac{B^2 d^2}{4\pi\mu\rho\eta\nu}, \tag{2}$$

where the coefficient of expansion $\alpha = T^{-1}$ for a gas, the magnetic diffusivity $\eta = (4\pi\mu\sigma)^{-1}$ and g is the gravitational acceleration, β the superadiabatic temperature gradient, d the depth of a convection cell, B the vertical magnetic field, μ the permeability, κ the thermal diffusivity, ν the kinematic viscosity and σ the electrical conductivity. In the Sun, ν is small and $Q \gg 1$; we assume that the onset of convection can be described by the linearized theory for a Boussinesq fluid contained between free boundaries (Chandrasekhar 1961). Then, for $\kappa < \eta$, convection occurs first as a monotonically growing instability at the critical Rayleigh number

$$R_c = \pi^2 Q; \tag{3}$$

the potential temperature difference across the cell is

$$\theta_c = \beta_c d = 2\pi^2 \left(\frac{\kappa}{\eta}\right) \frac{B^2}{8\pi\mu} \cdot \frac{T}{g\rho d}. \tag{4}$$

However, convection is only effective when the motion can dominate the field. This occurs when the buoyancy force balances the Lorentz force so that for adiabatic motion

$$\theta_e = \beta_e d \sim 2\pi^2 \frac{B^2}{8\pi\mu} \cdot \frac{T}{g\rho d}. \tag{5}$$

If, on the other hand, $\kappa > \eta$ then convection first appears as overstable oscillations, when

$$\theta_0 = \beta_0 d = 2\pi^2 \left(\frac{\eta}{\kappa}\right) \frac{B^2}{8\pi\mu} \cdot \frac{T}{g\rho d}. \tag{6}$$

These overstable modes correspond to standing Alfvén waves which gain energy from the unstable thermal stratification. Such oscillatory convection is inefficient compared with overturning motions. The latter correspond to monotonically growing instabilities, which first appear when $\beta \sim \beta_e$ (Danielson 1961, 1965; Weiss 1964a).

In the sun energy is carried by radiation, and the thermal diffusivity

$$\kappa = \frac{4acT^3}{3\bar{\kappa}\rho^2 c_p}, \tag{7}$$

where a is the radiation density constant, $\bar{\kappa}$ the mean opacity and c_p the specific heat. Values of κ computed using the program described by Baker & Temesvary

(1968) differ from those given by Danielson & Savage (1966); this discrepancy is probably due to our using more recent, and therefore higher, estimates of the opacity. The magnetic diffusivity is given approximately by

$$\eta = 3.10^{12}\, T^{-3/2}\ \mathrm{cm^2\ s^{-1}} \tag{8}$$

(Spitzer 1956). Fig. 1 shows κ and η as functions of depth in the convective zone: the conductivity drops rapidly, mainly owing to the increase in opacity caused by ionization, and $\eta > \kappa$ over the range 2000 km $< z <$ 20 000 km. The corresponding values within the flux rope do not differ significantly at depths below 2000 km, though η increases to 10^{10} cm^2 s^{-1} in the umbra.

In the region $z <$ 2000 km, $\kappa > \eta$ and convection sets in as overstable oscillations. Without rigid boundaries, linear disturbances travel as Alfvén waves with exponentially increasing amplitude; the non-linear motion corresponds to surges up and down along the field lines. Near the surface the product of the Rayleigh number and the Prandtl number (ν/κ) is of order unity. Radiative losses become

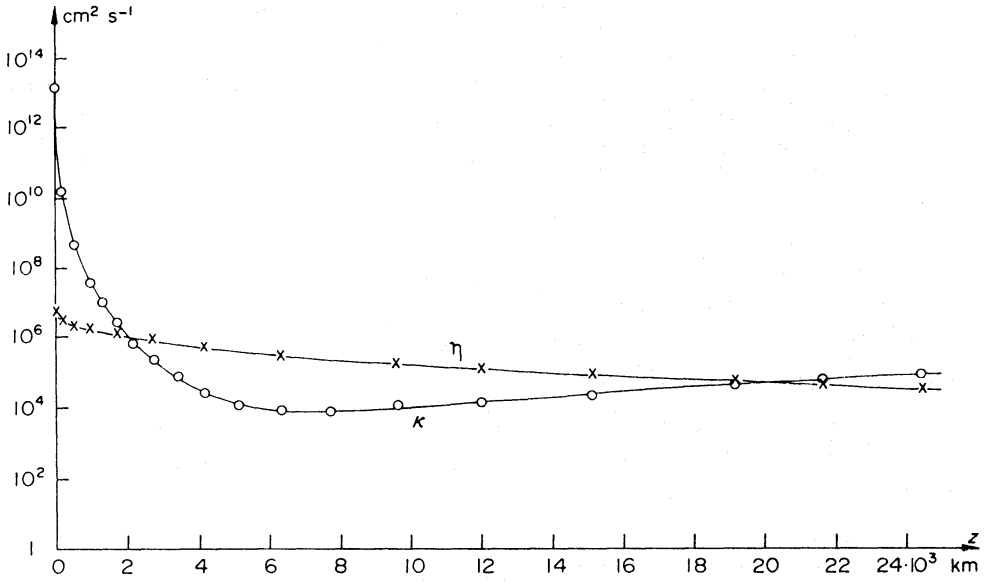

FIG. 1. *Variation of κ and η with depth in the upper part of the convective zone.*

important and the superadiabatic temperature gradient is too low for steady convection to take place (Danielson 1965).

Below 2000 km convection appears as a monotonically growing instability throughout the supergranular region, though non-linear effects may lead to finite amplitude oscillations (Weiss 1974). These non-linear oscillations should be stationary rather than travelling phenomena, and capable of transporting heat. At the onset of convection, cells are elongated but they rapidly become more isotropic as the Rayleigh number is increased.

Consider a flux tube with a vertical field that is independent of z. The difference between the external and internal gas pressures is equal to the magnetic pressure p_m. If p_m is constant, ρ must be the same inside and outside the flux rope, and the temperature difference between the flux rope and the external gas is

$$\Delta T = \frac{p_m}{p}\, T = \frac{T}{p}\, \frac{B^2}{8\pi\mu}. \tag{9}$$

From equation (4) convection should occur if the potential temperature difference θ across a layer of depth d within the flux rope exceeds the critical value θ_c. But, from (4) and (9),

$$\theta_c = 2\pi^2 \left(\frac{\kappa}{\eta}\right) \Delta T \frac{H_p}{d}, \tag{10}$$

where H_p is the pressure scale height. Now θ is the sum of the external potential temperature difference and the change in ΔT over the layer depth d; moreover the scale height for ΔT is the density scale height H_ρ, from (9), and $d \sim H_\rho$ also. Hence $\theta > \Delta T$ and a sufficient condition for convection to occur is that $\Delta T > \theta_c$ or, using (10), that $d/Hp > 2\pi^2(\kappa/\eta)$. From equation (5), the corresponding condition for convection to be efficient is that $d/H_p > 2\pi^2$. In the region between about 4000 and 10 000 km depth, $2\pi^2\kappa/\eta \approx 1$ (see Fig. 1) and $1 < (H_\rho/H_p) < 5/3$. Therefore $\theta_c \lesssim \theta \lesssim \theta_e$: some convection is present, though its efficiency is limited by the magnetic field.

The argument applies provided the radius of the cell is less than that of the flux rope itself. This does not hold for $z \gtrsim 10^4$ km. At this level external kinetic energy density also becomes equal to the internal magnetic energy density. Magnetic flux is concentrated by converging supergranular flow to produce a field that is strong enough locally to halt convection. This concentration maintains the flux rope and small scale convection can no longer occur.

It is therefore possible to distinguish three regions between the umbra of a long-lived sunspot and the underlying giant cells.

(i) At depths around 10 000–15 000 km the field is concentrated by local supergranular motion until large scale convection is suppressed. This process yields an equipartition field of about 3500 G; the actual field strength may be twice as large (Deinzer 1965; Peckover & Weiss 1973). Although no overturning motion can take place, Danielson & Savage (1968) have shown that mechanical energy may be transported upwards along the flux rope in the form of Alfvén waves; Wilson (1974b) has suggested that this Alfvén flux might be as high as 10^{10} erg cm^{-2} s^{-1}.

(ii) In the intermediate region (10 000 km $> z >$ 2000 km) convection is only partly inhibited by the field. The combination of small scale motions outside the flux rope and reduced convection within allows heat to be carried in laterally from the ambient supergranules and then transported upwards; this process may be augmented by the flux of Alfvén waves, which has been discussed by Wilson (1974b). If we assume that the observed flux of energy through the umbra is supplied entirely by convection, the associated velocities can be estimated. The convective heat transport

$$E \sim \tfrac{1}{2} c_p \rho w \theta, \tag{11}$$

where w is the vertical component of the velocity $\mathbf{u}$. At 6000 km depth $\Delta T \approx 25$ K and $c_p \approx 9.10^8$ ergs g^{-1} K^{-1}; in the ambient convective zone $\beta \sim 0{\cdot}01$ K km^{-1}. If E is the umbral flux of 10^{10} ergs cm^{-2} s^{-1} and $\theta \sim 50$ K then $w \sim 20$ m s^{-1}. The vertical dimension of the eddy $d \sim H_\rho \sim 2000$ km; its horizontal radius would be similar. The superadiabatic gradient $\beta \sim 0{\cdot}03$ K km^{-1}, while the critical value $\beta_c \approx 0{\cdot}01$ K km^{-1}, and the ratio of the kinetic to the magnetic energy density, $4\pi\mu\rho w^2/B^2 \sim 10^{-3}$. The presence of convective motion provides a local eddy diffusivity which is comparable with that outside the flux rope.

(iii) The shallow region above about 2000 km depth limits the energy flux through the umbra. It is only here that the sunspot is significantly cool. If we adopt a Wilson depression of 500 km, the temperature difference between the umbra at $\tau = 1$ and the undisturbed convective zone is 9000 K; at 2000 km $\Delta T = 500$ K. The magnetic field suppresses convection and energy is transported either by columns rising and falling parallel to the field or by partially trapped hydromagnetic waves. The latter correspond to overstable convection, which has been investigated by Danielson (1961, 1965), Musman (1967), Danielson & Savage (1968), and Savage (1969). The observed microturbulent velocities (~ 2 km s^{-1}) may be related to this process, though umbral dots are probably a separate phenomenon. They appear sporadically and could be caused by penetration of convection from the unstable into the stable region.

5. EVOLUTION OF A SUNSPOT

We now put forward a unified account of the physical processes involved in the growth and decay of sunspots. Though parts are inevitably speculative, the whole description is consistent with the observations summarized in Section 2. The crucial phase of slow decay will be discussed in greater detail in Section 6.

The natural state of magnetic flux in a convective zone is to be concentrated into ropes (Weiss 1964b, 1966, 1969). These ropes (which are not necessarily vertical) are formed by the expulsion of magnetic fields from convection cells. Examples of this process can be observed in the Sun: magnetic knots are formed between granules, sunspots appear between supergranules and active longitudes map the boundaries of giant cells (Howard 1971).

Consider a flux rope formed in the deep convective zone. Rising material between adjacent giant cells can carry a stitch upwards towards the surface (Schmidt 1968; Ponomarenko 1970). The stitch will continue to rise owing to magnetic buoyancy (Parker 1955). This rising flux loop may form the nucleus of a new supergranule or else it may be picked up by an existing supergranule. In either case it will emerge through the surface at the centre of a supergranule, forming an arch filamentary system. The cellular motion rapidly sweeps the feet of the arch to the edge of the supergranule. Various hydromagnetic models of this process have been described by Parker (1963), Clark (1965), Weiss (1966) and Clark & Johnson (1967).

Two separate processes then contribute to the formation of a spot (Ponomarenko 1972a). First, flux is continually concentrated at a junction in the supergranular network. Secondly, the concentrated field halts convection; once the flux concentration becomes too large to be heated by radiation, the gas cools and sinks while the field strength increases to form a new configuration in which magnetic stresses balance the external pressure. This pressure provides the stabilizing collar which was discussed in Section 3. The cooled region forms a pore which develops a penumbra and becomes a sunspot as the flux increases (Simon & Weiss 1970).

As the flux rope continues to emerge its feet move further apart. The sunspots follow these feet, moving from corner to corner of the supergranular network. Thus the separation between leader and follower spots of a bipolar group continues to increase. As more flux appears it is concentrated by the supergranules. The

spots continue to grow rapidly and to move apart until all the flux has emerged and the active region has reached its maximum extent.

During the growth phase supergranules concentrate the flux down to a depth of about 10 000 km (Simon & Weiss 1968). For about 5000 km below that the flow diverges, causing a swelling in the flux rope (Wilson 1968; Ponomarenko 1972a, b). The converging flow descends around the sunspot and cools the region at its base. But the spreading penumbral field extends far beyond the flux rope and covers part of the adjacent supergranules. The area over which heat is transmitted to the photosphere is therefore reduced and the efficiency of supergranular convection is impaired. As a result, the region around the base of a spot is insufficiently cooled. The gas in this region heats up and eventually rises, reversing the flow pattern in the neighbourhood of the spot. This reversal can break up the flux rope (Ponomarenko 1972b); umbrae often develop light bridges and then split (Wilson 1968), and many sunspots are destroyed within a few days after their flux has reached a maximum. However, some large spots, after an initial loss of flux, achieve a quasistationary configuration and decay slowly over several rotations of the Sun.

Clearly, sunspots can be destroyed by supergranules just as pores are broken up by granules. What determines whether a particular spot will survive? We conjecture that this depends on the form of the flux rope beneath the spot. A sunspot will be preserved if the reversed flow can form an annular convection cell (whose upper surface forms the moat) around it. This is possible only if there is a fairly uniform vertical field at depths of 10 000 km and more: if the flux rope is inclined or split, it will be torn apart. A systematic difference in inclination could then explain the survival of the leading rather than the following spot in a bipolar group.

Reversal of the flow around a sunspot terminates its growth in flux and area. The moat should be associated only with slowly decaying spots. Once the spot is stationary, the temperature below it can systematically increase and the flow is more likely to reverse. If the annular cell forms earlier, it moves as a snow plough with the spot, sweeping away any magnetic flux or plages that it may encounter.

We now consider the slow decay of long-lived spots. Although magnetic flux emerging through a supergranule is carried to its boundaries within a few hours the annular cell cannot reverse this process on the same time scale. The field is isolated in a region where it is strong enough locally to inhibit convection and the large scale motion does not penetrate into the flux rope. The rate of decay is limited by the rate at which flux can leak from the rope into the annular cell. A detailed model of this process will be described in the next section and related to observations of moving magnetic features in Section 8.

The annular cell remains throughout the slow decay phase. Flux that has escaped from the sunspot is rapidly carried across the moat and slowly dispersed as magnetic knots that move over into nearby supergranules. However, these flux tubes may still be part of the main flux rope at depths below 10 000 km, where the main cellular flow converges on the rope. The annular cell will persist so long as the pattern of convection is dominated by the insulating effect of the shallow penumbra. As the spot decays its area decreases. Eventually, when the radius of the spot is less than about 10 000 km, neighbouring supergranules break into the moat and the annular cell is destroyed. The flux rope is torn apart

and the sunspot disappears within a few days. Its flux is slowly distributed, by a random walk process, among the supergranules. Nevertheless, the original flux rope still remains in the deep convective zone. Another rising stitch can form a new active region, whose position is fixed by the pattern of giant convection cells. Elongation of these cells parallel to the rotation axis of the Sun establishes the active longitudes (Busse 1973).

6. SLOW DECAY

A long-lived sunspot may survive for several solar rotations while its magnetic flux and area decrease. The most striking feature of this slow decay is that the sunspot area A decreases linearly with time (Royal Greenwich Observatory 1925, Cowling 1946; Bumba 1963; Bray & Loughhead 1964; Gokhale & Zwaan 1972). Although individual spots fluctuate, the average decay rate for 60-day spots is constant throughout most of their lifetime and

$$\frac{dA}{dt} \approx -3.10^{12}\ \mathrm{cm^2\ s^{-1}} \tag{12}$$

(Royal Greenwich Observatory 1925). Bumba (1963) found a constant minimum decay rate for long-lived spots; however, its value was about half that given in (12). Since the magnetic flux Φ in a large sunspot is directly proportional to its area these observations imply that $d\Phi/dt$ is also constant (Cowling 1946; Bray & Loughhead 1964). In this section we put forward a model which explains this constant decay rate.

It has been suggested (Simon & Leighton 1964; Schmidt 1968) that magnetic flux is chipped off around the edge of the sunspot. Although the moving magnetic features leaving the sunspot are transported by the supergranulation this process cannot be governed by the supergranulation alone. Any such process acting locally around the periphery of a sunspot leads to a decay rate proportional to the circumference of the spot so that $dA/dt \propto A^{1/2}$, which contradicts the observations. A constant decay rate implies that it must be easier to peel off flux tubes from the main rope as A decreases. This could be achieved by assuming ohmic losses in a boundary layer whose thickness varies as the radius of the spot (Gokhale & Zwaan 1972). However it is implausible that a thin localized layer (less than 10^{-4} of the umbral radius) should vary systematically with the global dimension of the spot.

A constant decay rate apparently needs a process which acts throughout the flux rope below the spot. It is striking that dA/dt has the dimensions of a diffusivity. At depths of 2000–12 000 km the radiative conductivity and the resistivity are both small ($\kappa \sim 10^4\ \mathrm{cm^2\ s^{-1}}$, $\eta \sim 10^6\ \mathrm{cm^2\ s^{-1}}$); on the other hand, estimates of the convective eddy diffusivity lie within an order of magnitude of the value of dA/dt in (12). We can distinguish between large scale (supergranular) convective motions, which do not penetrate into the flux rope, and small scale motion inside and outside the flux tube, which allows lines of force to leak outwards. In Section 4 we estimated that at depths around 6000 km there could be eddies inside the flux rope with a radius of about 2000 km and speeds around 20 m s^{-1}. Similar motions are present in the annular cell: if they carry, say, 10 per cent of the total energy they may have speeds of up to 100 m s^{-1}. Thus there exists a roughly uniform eddy diffusivity, inside and outside the flux rope, which enables small flux tubes to escape from it.

The cylindrical flux rope is surrounded by an annular region corresponding to the moat, as shown schematically in Fig. 2. In order to describe the decay process we distinguish between three layers. In layer I, at the base of the supergranular region, the inflow provides a collar which concentrates magnetic flux. In layer II both the field and the large scale supergranular motion around it are approximately vertical. However, the concentrated field remains strong enough to exclude large scale convection from the inner portion of the rope. Within 3000 km of the surface,

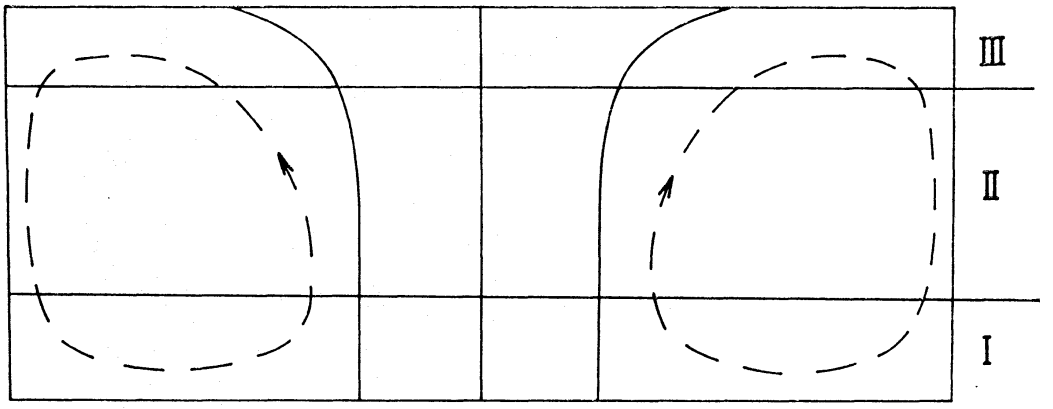

FIG. 2. *Schematic diagram of a sunspot (vertical scale exaggerated by two). In layer I (10–15 000 km) flux is concentrated by the supergranular flow. In layer II (3–10 000 km) the field is nearly vertical and diffuses out into the annular supergranule. In region III the flow is predominantly horizontal and flux tubes leave the sunspot.*

in layer III, there is a large scale horizontal outflow. Despite the collar maintained by external pressure, flux tubes leave the sunspot at its boundary, where the field too is horizontal.

We assume that the spot decays through the eddy diffusivity resulting from small scale convection in region II of Fig. 2, at depths around 6000 km. As lines of force diffuse outwards into the annular cell they participate in its large scale motion. At this level the velocity is vertical but near the surface, in region III, gas flows radially outwards from the sunspot, carrying magnetic flux across the moat. Thus only part of the flux concentrated in layer I emerges through the sunspot. In region II there is a cylindrical surface separating the main flux rope that continues through the sunspot from the flux outside that takes part in supergranular motion. On this bounding surface there is a balance between magnetic stresses and the effects of convection. The strength of the convection does not change significantly with time during the slow decay phase, nor does it vary much with height in region II. It is therefore reasonable to assume that the boundary is characterized by a constant magnetic field B_c such that $B < B_c$ in the convecting region. We now construct a simplified model of decay owing to diffusion across this boundary.

Suppose that the magnetic field in layer II is everywhere vertical and independent of depth, and that field lines diffuse in the radial direction (Meyer & Schmidt 1972). Let r be the distance from the axis of the sunspot and $B(r, t)$ the vertical magnetic field. Then, for a constant *eddy* diffusivity η,

$$\frac{\partial B}{\partial t} = \frac{\eta}{r}\frac{\partial}{\partial r}\left(r\frac{\partial B}{\partial r}\right), \tag{13}$$

since there is no large scale motion across the field lines.

After a time any concentrated field will tend towards the fundamental Gaussian solution

$$B(r, t) = \frac{\Phi_0}{4\pi\eta t} \exp\left(-\frac{r^2}{4\eta t}\right), \tag{14}$$

where Φ_0 is the total flux. All the field lines for which $B > B_c$ intersect the photosphere within the sunspot. For $B < B_c$ the lines of force follow the supergranular convective motion and are drawn across the moat. Hence the sunspot flux

$$\Phi = \int_0^{r_c} 2\pi B r dr, \tag{15}$$

where $r_c(t)$ is the radius of the main flux rope so that $B(r_c, t) = B_c$. Then, from (14) and (15),

$$\Phi = \Phi_0\left(1 - \exp\left(-\frac{r_c^2}{4\eta t}\right)\right) = \Phi_0 - 4\pi\eta B_c t. \tag{16}$$

It follows immediately that the decay rate

$$\frac{d\Phi}{dt} = -4\pi\eta B_c \tag{17}$$

and is constant.

So far the discussion refers only to region II. Observations are confined to the upper surface of region III. The magnetic field in the visible sunspot is determined by the need to maintain hydrostatic equilibrium and differs from that in layer II; in particular, the observed central field $B_m \neq B(0, t) \propto 1/t$. In fact, B_m remains constant for most of a spot's lifetime (Cowling 1946) and the flux is related to the measured area by

$$\Phi \approx 0{\cdot}4\, B_m A \tag{18}$$

(Bray & Loughhead 1964). From (17) and (18) we find that

$$\frac{dA}{dt} \approx -10\pi\eta \frac{B_c}{B_m}. \tag{19}$$

Both B_m and dA/dt are determined by observation. The critical field B_c cannot be measured but the diverging field lines in a sunspot suggest that B_c lies between the magnitude of the field at the edge of the penumbra and that at the edge of the umbra. Alternatively, B_c can be estimated by assuming a balance between magnetic energy and the kinetic energy of supergranular convection, so that

$$\frac{B_c^2}{8\pi\mu} = \tfrac{1}{2}\rho u^2. \tag{20}$$

Taking $\rho = 2.10^{-4}$ g cm^{-3}, $u = 3.10^4$ cm s^{-1}, we obtain $B_c \approx 1500$ G. We shall assume that $B_c/B_m = \frac{1}{2}$. Then, from equation (19), the observations indicate that

$$\eta \approx 2.10^{11} \text{ cm}^2 \text{ s}^{-1}. \tag{21}$$

This value must be compared with the effective diffusivity for the vertical field in layer II.

In order to estimate the eddy diffusivity we need a model of the turbulent diffusion process. We consider a convective eddy with horizontal radius R and lifetime τ and suppose that during the eddy's lifetime all the flux emerging from its upper surface is swept to its boundary. The mean square displacement of a line of force is

$$d^2 = \frac{1}{R^2}\int_0^R (R-r)^2 r dr = \frac{1}{6}R^2. \tag{22}$$

After a time t the mean square displacement is $d^2 t/\tau$. For the Gaussian field distribution of equation (14) the mean square displacement of a flux element after time t is

$$\frac{1}{\Phi_0}\int_0^\infty r^2 B 2\pi r dr = 4\eta t. \tag{23}$$

Comparing these two values, we find that

$$\eta = \frac{1}{24}\frac{R^2}{\tau}. \tag{24}$$

A similar result for fully developed turbulence was obtained by Parker (1971). For an eddy with characteristic speed v the lifetime is approximately the turnover time $\tau_0 = R/v$. Typical values of R, τ and v for supergranules, granules and the small scale turbulence at a depth of about 6000 km are given in Table II, together with the corresponding estimates of η from (24). The effective diffusivity for small scale convection is consistent with the value required by (21).

Of course, we have only considered a very simple model of the decay process. For instance we have ignored the vertical variation of the field as it diffuses. Again we have neglected any dependence of η on the field strength. However, the decay is dominated by diffusion at the interface where $B \sim B_c$ and should not be too sensitive to variations of η.

TABLE II

Estimated diffusivities for magnetic fields

	R (cm)	v (cm s^{-1})	τ (s)	η (cm^2 s^{-1})
Supergranules	$1{\cdot}5\times10^9$	4×10^4	7×10^4	$1{\cdot}3\times10^{12}$
Granules	$1{\cdot}0\times10^8$	2×10^5	5×10^2	8×10^{11}
Small-scale convection	2×10^8	1×10^4	2×10^4	8×10^{10}

The essential features of this model are the separation between the flux rope and large scale convection and the coupling of slow decay (governed by turbulent diffusion) with rapid transport of flux across the moat. We have illustrated this behaviour by carrying out a number of simplified numerical experiments which will be described in the next section. The decay process outlined here is entirely consistent with observations, particularly those of Harvey & Harvey (1973). Evidence for the diffusion of flux elements within a sunspot might be derived from Muller's (1973) observations of bright features migrating inwards to the umbral–penumbral boundary with a lifetime of about 3 hr.

7. A NUMERICAL MODEL

During the slow decay phase, when the sunspot lies at the centre of an annular convection cell, we have asserted (i) that the motion is excluded from the region where the magnetic field exceeds some critical value B_c; (ii) that the sunspot decays on a time scale slow compared with the turnover time for the cell; (iii) that the decay rate is determined by turbulent diffusion acting throughout the flux rope; and (iv) that once field lines have diffused into the convecting region they are rapidly swept aside by the motion. This behaviour can be illustrated by numerical experiments using a highly simplified model, with the turbulent diffusion represented by an ordinary resistivity.

The equations governing hydromagnetic convection in a Boussinesq fluid can be expressed in dimensionless form by adopting d as unit of length, T_0 as unit of temperature, $(d/g\alpha T_0)^{1/2}$ as unit of time and $(4\pi\mu g\rho\alpha T_0 d)^{1/2}$ as unit of magnetic field. Then

$$\frac{\partial \mathbf{B}}{\partial t} = \nabla \wedge (\mathbf{u} \wedge \mathbf{B}) + \eta \nabla^2 \mathbf{B}, \tag{25}$$

$$\frac{\partial T}{\partial t} = -\nabla.(T\mathbf{u}) + \kappa \nabla^2 T, \tag{26}$$

$$\frac{\partial \mathbf{u}}{\partial t} = -\nabla.(\mathbf{uu}) - T\mathbf{g} - \nabla p + (\nabla \wedge \mathbf{B}) \wedge \mathbf{B} + \nu \nabla^2 \mathbf{u}, \tag{27}$$

$$\nabla.\mathbf{u} = 0. \tag{28}$$

These equations can be solved numerically for two-dimensional flow in a plane horizontal layer (Peckover & Weiss 1973), using methods described by Moore, Peckover & Weiss (1973).

We consider flow between horizontal planes perpendicular to the z-axis, with $\mathbf{u}$ and $\mathbf{B}$ confined to the xz-plane, and independent of y, and assume periodicity in the x-direction. Then equations (25)–(28) are solved in the square region $0 < x < 1$, $0 < z < 1$, subject to boundary conditions

$$B_x = 0 \quad (x = 0, 1;\ z = 0, 1),$$
$$T = 0 \quad (z = 1), \qquad T = \beta \quad (z = 0), \qquad \frac{\partial T}{\partial x} = 0 \quad (x = 0, 1), \tag{29}$$

while the normal component of $\mathbf{u}$ and the tangential viscous stress vanish on all boundaries.

The initial conditions are chosen to simulate the development of a supergranule around a previously concentrated flux rope. The 'sunspot' is represented by a uniform vertical field in the region $|x| < \Delta$, the temperature is uniformly stratified and convection is started with a clockwise rotating eddy in the region $\Delta < |x| < 1$. At time $t = 0$

$$\begin{aligned} \mathbf{B} &= (0, 0, B_0) \quad (0 \leqslant x < \Delta) \\ &= 0 \quad (\Delta < x \leqslant 1) \end{aligned} \tag{30}$$

and

$$\begin{aligned} \mathbf{u} &= 0 \quad (0 \leqslant x < \Delta) \\ &= \nabla \wedge \left[\frac{U}{\pi} \sin \frac{\pi(x-\Delta)}{(1-\Delta)} \sin \pi z\, \mathbf{e}_y \right] \quad (\Delta < x \leqslant 1), \end{aligned} \tag{31}$$

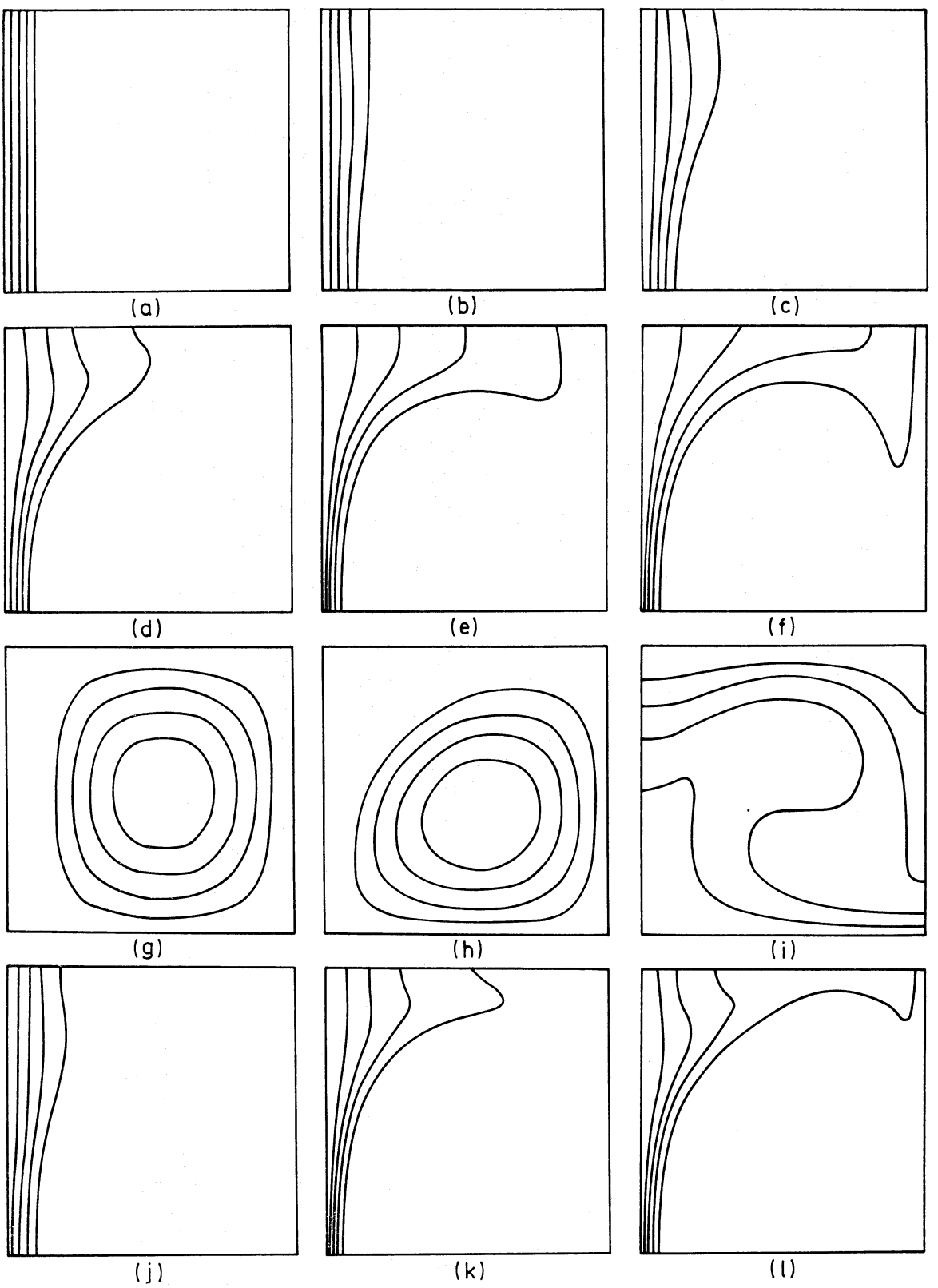

FIG. 3. *Numerical experiments with* $R = 2{\cdot}5 \times 10^4$, $\kappa = 0{\cdot}04$, $\nu = 0{\cdot}01$. *Lines of force for* $\eta = 0{\cdot}01$ *at* (*a*) $t = 0$, (*b*) $t = 0{\cdot}44$, (*c*) $t = 0{\cdot}88$, (*d*) $t = 1{\cdot}32$, (*e*) $t = 1{\cdot}76$, (*f*) $t = 2{\cdot}20$. *Results for* $\eta = 0{\cdot}005$: (*g*) *streamlines at* $t = 0$, (*h*) *streamlines at* $t = 2{\cdot}54$, (*i*) *isotherms at* $t = 2{\cdot}64$; *lines of force at* (*j*) $t = 0{\cdot}88$, (*k*) $t = 1{\cdot}76$, (*l*) $t = 2{\cdot}64$.

where $\mathbf{e}_y$ is a unit vector in the y-direction. Values of the various parameters are then chosen to produce the behaviour of a sunspot.

Fig. 3 shows some results of these numerical experiments, with $R = 2{\cdot}5 \times 10^4$, $\kappa = 0{\cdot}04$, $\nu = 0{\cdot}01$, $\Delta = 0{\cdot}125$, $B_0 = 1{\cdot}5$, $U = 0{\cdot}5$. The initial magnetic field, shown in Fig. 3(a), diffuses outwards and is then drawn across the upper boundary of the cell. Fig. 3(b)–(f) show this process with $\eta = 0{\cdot}01$ ($Q = 2{\cdot}25 \times 10^4$).

By $t = 2{\cdot}20$ the 'spot' is mainly dispersed. Another set of results, obtained with $\eta = 0{\cdot}005$, is shown in Fig. 3 (j)–(l): reducing the resistivity slows down the decay and the flux is still concentrated when $t = 2{\cdot}64$. The initial velocity, whose streamlines are shown in Fig. 3(g), develops into the asymmetric cell of Fig. 3(h), while the corresponding temperature field is shown in Fig. 3(i). The maximum speed increases to about 2·2 and the strength of the concentrated field rises to 3·3. The turnover time τ_0 (half the period of a full rotation of the eddy) is 0·5–0·75 and the results shown cover a period $0 < t \lesssim 4\tau_0$.

The subsequent behaviour is more complicated. In the flux tube the isotherms lag behind the rising plume, as can be seen in Fig. 3(i). The resulting density gradient generates a countercell in the top left-hand corner, which at first helps to confine the field but later develops to split the flux tube and so finally produces a steady symmetrical configuration. This has no analogue in a sunspot where the reduced gas pressure decreases ρ within the flux tube. In the Boussinesq model dynamical equilibrium is maintained by the lateral boundary conditions.

These computations confirm the qualitative features of our model. Fig. 3(h) shows that the flow does not penetrate into the flux rope and Fig. 3(a)–(f) demonstrate the combination of slow diffusion and rapid advection that destroys the spot. The differences between Fig. 3(c) or (e) and 3(j) or (k) shows that the decay rate is determined by diffusion. This appears more clearly from Fig. 4: the profiles of the vertical magnetic field at $z = 0{\cdot}75$, $t = 0{\cdot}88$ have similar shapes and are approximately Gaussian. The original resistive time scale $\Delta^2/4\eta = 0{\cdot}4$, 0·8 when $\eta = 0{\cdot}01$, 0·005 so diffusion acts throughout the flux rope. It is clear also that

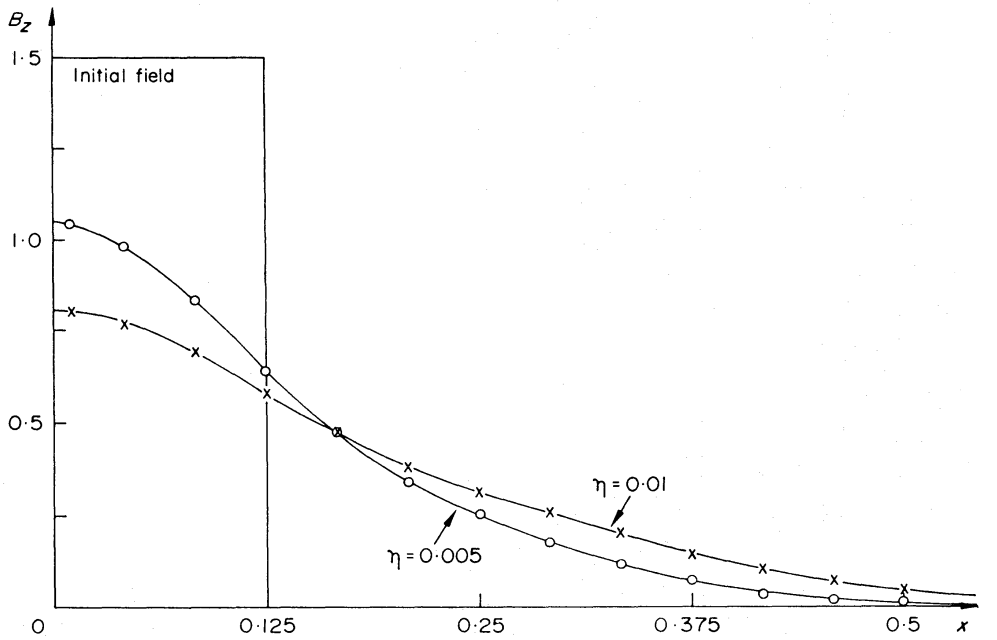

FIG. 4. *Profiles of the vertical component of* **B** *at* $z = 0{\cdot}75$, $t = 0{\cdot}88$ *for* $\eta = 0{\cdot}01$ *and* $\eta = 0{\cdot}005$, *compared with the initial field.*

the decay time can be much greater than the turnover time, though the ratio t/τ_0 is much less than for a long lived sunspot.

A constant decay rate requires a cylindrical configuration and is not to be expected in this geometry. However, the numerical experiments include the effects of vertical as well as horizontal variations in the field. Consequently, the critical field B_c at the interface between the flux rope and the eddy is not uniquely defined. Inspection of Fig. 3 shows that the streamlines and lines of force at this interface run perpendicular to the diagonal from the top left-hand corner. The transverse component of **B** evaluated along the diagonal $x-z=1$ reaches a relative maximum as the field becomes aligned with the flow. Its value then drops sharply. This maximum coincides with a sudden increase in $|\mathbf{u}|$ and a corresponding maximum of $|\text{curl } \mathbf{u}|$, and it is a convenient measure of B_c. From the calculations described above $B_c = 0{\cdot}70 \pm 0{\cdot}03$. In a different series of runs with $B_0 = 1{\cdot}0$, $1{\cdot}5$, $2{\cdot}0$ and $R = 5.10^4$, $\kappa = 0{\cdot}02$, $\nu = 0{\cdot}01$, $\eta = 0{\cdot}005$ for $t \leq 4{\cdot}2$, the position of the maximum lay in the range $0{\cdot}19 \leq x \leq 0{\cdot}35$ and the enclosed flux varied by a factor of 3; yet $B_c = 0{\cdot}61 \pm 0{\cdot}06$. The difference between the two values of B_c corresponds to different strengths of convection in the two series of numerical experiments. For the first series the rms velocity $\bar{U} = 1{\cdot}27$; for the second series $\bar{U} = 1{\cdot}08$. The ratios $B_c/\bar{U}$ are $0{\cdot}55$ and $0{\cdot}57$, respectively. Throughout these computations the critical field, when suitably normalized, is amazingly constant. This result strongly supports the assumption of a constant value for B_c in the model described in the preceding section.

Although the computational model is drastically simplified, it reproduces many qualitative features of the slow decay process. Moreover, the four crucial features of our model for this process, mentioned at the beginning of this section, are all verified by the numerical experiments.

8. MOVING MAGNETIC FEATURES IN THE MOAT

The field outside a real sunspot is discontinuous, unlike that in the numerical model described above. Turbulent diffusion removes small flux tubes which are immediately carried away by the large-scale cellular motion, to appear as moving magnetic features in the moat. These features generally occur in pairs with opposite polarity; successive pairs tend to follow the same path across the moat and presumably correspond to kinks travelling along an underlying flux rope (Harvey & Harvey 1973). The separation between pairs and the fact that they can appear well away from the penumbra (Vrabec 1971) suggest that they may be produced when the flux rope is distorted by granules. Features with opposite polarity apparently move about 7 per cent faster than those with the same polarity; this could be caused by spreading of the kink like a miniature arch filamentary system. The average velocity of moving magnetic features is about 1 km s^{-1}, which is greater than the velocity obtained from Doppler spectroheliograms; this difference is consistent with the kinks moving outwards, with the Alfvén velocity, relative to the streaming gas.

There are two possible orientations in which flux can be carried away from a sunspot: head first or feet first, like a drunkard or a corpse. These two possibilities, which depend on whether the flux is removed at the photosphere or at depth, are illustrated in Fig. 5. The model of Fig. 5(a) was proposed by Harvey & Harvey (1973) and is consistent with the computations illustrated in Fig. 3.

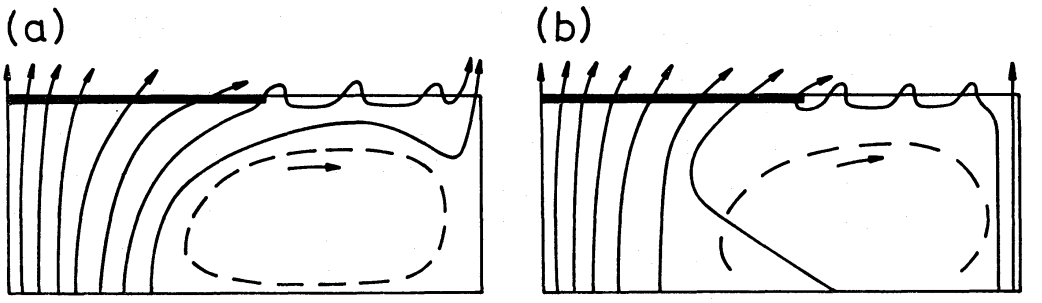

FIG. 5. *Flux loss from a sunspot. (a) Flux tubes leave the penumbra at the surface but remain part of the flux rope at depth. (b) Flux tubes leave the flux rope at depth before being removed from the penumbra. Solid lines represent magnetic field; broken lines represent streamlines.*

At a depth of several thousand kilometres small tubes escape from the main flux rope and take part in the supergranular motion. The field in these tubes no longer impedes convection and enough energy can be carried along them to overcome the stabilizing effect of the collar. The large scale motion then carries these flux tubes out of the sunspot and across the moat to join the surrounding network. The submerged flux tubes follow the streamlines and are nearly horizontal. While they are near the surface granules will bring up kinks which can be observed as moving magnetic features. Gradually the field lines will diffuse deeper into the convective cell and cease to appear in the moat. The gross flux observed by the Harveys corresponds to the formation of about four kinks over a period of approximately 20 hr. Thus an individual flux tube sinks below the level where granules originate in a time comparable with the turnover time for the annular convection cell itself.

In this model flux tubes remain attached to the main rope at depths around 12 000 km. An alternative possibility is that tubes first become detached from the rope at depths of order 12 000 km, as suggested by Wilson (1973) and illustrated in Fig. 5(b). Eddy diffusion still takes place between 2000 and 12 000 km. As a flux tube diffuses into the surrounding cell it is swept up by the flow. Some twisting and buckling occurs as the top of the tube is detached from the collar at the surface and these kinks will still be evident in the tube when it subsequently appears at the photosphere.

The most significant difference between the two models is that in the first flux tubes leave the penumbra fairly readily once they have separated from the rope below; in the second they are dragged through the collar by the large scale motion. Pairs of magnetic features have opposite polarity in Fig. 5(a) and (b); observations can therefore establish which model is correct. At present the results are uncertain. Magnetic features frequently appear close to the penumbra but those with opposite polarity to the sunspot tend to be formed further out. Harvey (private communication) has pointed out that Vrabec's magnetic spectroheliograms (see Harvey 1971, Plate 3) seem to show pairs of features with those of opposite polarity as leaders. These results marginally favour the model of Fig. 5(a).

9. DISCUSSION

The main premise of this paper has been that the evolution of sunspots must be understood in terms of the effect of convection on ropes of magnetic flux. This approach requires both a model of the flux rope beneath a sunspot and a

description of the convective zone. The growth and decay of sunspots can then be related to supergranular convection, though photospheric fields outside sunspots are concentrated into knots, with a small scale which is determined by the granulation.

Further observations are needed to confirm our description of a sunspot's evolution. Harvey & Harvey (1963) found moving magnetic features only near decaying sunspots with a moat. The size of the spot was not important, nor was it necessary for there to be a penumbra. Is the moat invariably associated with slow decay? And what determines whether a moat is formed? Individual magnetic features are difficult to observe but it would be valuable to make a careful study of their polarities around one spot. Does the first knot of a sequence have the same polarity as the spot and is it followed by pairs with alternating polarities? Do the knots remain in the network around the moat or does the flux spread away from the annular cell during the lifetime of the spot? Detailed studies of sunspots might show whether field lines diffuse to and fro and whether magnetic flux moves with the bright grains found by Muller (1973). It may be possible to clarify the relations between umbral dots and deep-seated convection.

We have supposed that sunspots are axially symmetric and surrounded by an annular convection cell. This ideal configuration is seldom approached. Moats are frequently incomplete and this lack of symmetry may be responsible for discrepant values of the observed decay rate. In order to improve the theory outlined here more detailed models have to be constructed. We need a better understanding of the effects of compressibility on convection in the Sun. Deinzer's (1965) procedure for computing sunspot models could be elaborated to include a more realistic description of convection in a magnetic field. And there is, as yet, no proper theory of the inhomogeneous penumbra. With these models a less schematic description of the slow decay phase would be possible. Finally, we have concentrated on individual sunspots. A more complete theory would describe the evolution of an active region. A rising flux tube spreads out and becomes distorted owing to differential rotation. This behaviour should explain both the proper motions of sunspots and the dominance of the leading spot (Ponomarenko 1970).

ACKNOWLEDGMENTS

We wish to thank Dr J. Harvey for correspondence concerning his results and Professor T. G. Cowling for his helpful comments on our manuscript. We are also grateful for discussions with Dr U. Anzer, Professor L. Biermann, Dr E. N. Frazier, Dr D. O. Gough, Dr J. Harvey, Dr K. Harvey, Dr N. R. Sheeley, Dr D. Vrabec and Professor C. Zwaan.

F. Meyer, H. U. Schmidt and N. O. Weiss:
Max-Planck-Institut für Physik und Astrophysik, München

P. R. Wilson:
Department of Applied Mathematics, University of Sydney

N. O. Weiss:
On leave from *Department of Applied Mathematics and Theoretical Physics, University of Cambridge*

Received in original form 1974 *April* 18

REFERENCES

Baker, N. & Temesvary, S., 1966. *Tables of convective stellar models*, NASA, New York.
Beckers, J. M. & Schröter, E. H., 1968. *Sol. Phys.*, **4**, 303.
Biermann, L., 1941. *Vierteljahrschr. Astr. Ges.*, **76**, 194.
Bray, R. J. & Loughhead, R. E., 1964. *Sunspots*, Chapman and Hall, London.
Bruzek, A., 1967. *Sol. Phys.*, **2**, 451.
Bruzek, A., 1969. *Sol. Phys.*, **8**, 29.
Bumba, V., 1963. *Bull. astr. Inst. Czech.*, **14**, 91.
Busse, F. H., 1973. *Astr. Astrophys.*, **28**, 27.
Chandrasekhar, S., 1961. *Hydrodynamic and hydromagnetic stability*, Clarendon Press, Oxford.
Chitre, S. M., 1963. *Mon. Not. R. astr. Soc.*, **126**, 431.
Clark, A., 1965. *Phys. Fl.*, **7**, 1455.
Clark, A. & Johnson, A. C., 1967. *Sol. Phys.*, **2**, 433.
Cowling, T. G., 1946. *Mon. Not. R. astr. Soc.*, **106**, 218.
Cowling, T. G., 1957. *Magnetohydrodynamics*, Interscience, New York.
Danielson, R. E., 1961. *Astrophys. J.*, **134**, 289.
Danielson, R. E., 1965. *Stellar and solar magnetic fields*, p. 314, ed. R. Lüst, North Holland, Amsterdam.
Danielson, R. E. & Savage, B. D., 1968. *Structure and development of solar active regions*, p. 112, ed. K. O. Kiepenheuer, Reidel, Dordrecht.
Deinzer, W., 1965. *Astrophys. J.*, **141**, 548.
Frazier, E. N., 1972. *Sol. Phys.*, **26**, 130.
Gokhale, M. H. & Zwaan, C., 1972. *Sol. Phys.*, **26**, 52.
Harvey, J., 1971. *Publ. astr. Soc. Pacific*, **83**, 539.
Harvey, K. & Harvey, J., 1973, *Sol. Phys.*, **28**, 61.
Howard, R., 1971. *Publ. astr. Soc. Pacific*, **83**, 550.
Krat, V. A., Karpinsky, V. N. & Pravdjuk, L. M., 1972. *Sol. Phys.*, **26**, 305.
Meyer, F. & Schmidt, H. U., 1968. *Mitteilungen Astr. Ges.*, **25**, 194.
Meyer, F. & Schmidt, H. U., 1972. *Mitteilungen Astr. Ges.*, **32**, 173.
Moore, D. R., Peckover, R. S. & Weiss, N. O., 1973. *Comp. Phys. Comm.*, **6**, 198.
Muller, R., 1973. *Sol. Phys.*, **29**, 55.
Musman, S., 1967. *Astrophys. J.*, **149**, 201.
Mykland, N., 1973. *Sol. Phys.*, **28**, 49.
Parker, E. N., 1955. *Astrophys. J.*, **121**, 491.
Parker, E. N., 1963. *Astrophys. J.*, **138**, 552.
Parker, E. N., 1971. *Astrophys. J.*, **163**, 279.
Peckover, R. S. & Weiss, N. O., 1973. *Comp. Phys. Comm.*, **4**, 339.
Piddington, J., 1973. *Sol. Phys.*, **31**, 229.
Ponomarenko, Yu. B., 1970. *Astr. Zh.*, **47**, 98 (*Astr. J.*, **14**, 78, 1970).
Ponomarenko, Yu. B., 1972a. *Astr. Zh.* **49**, 148 (*Astr. J.*, **16**, 116, 1972).
Ponomarenko, Yu. B., 1972b. *Astr. Zh.*, **49**, 568 (*Astr. J.*, **16**, 460, 1972).
Royal Greenwich Observatory, 1925. *Mon. Not. R. astr. Soc.*, **85**, 553.
Savage, B. D., 1969. *Astrophys. J.*, **156**, 707.
Schlüter, A. & Temesvary, S., 1958. *Electromagnetic phenomena in cosmical physics*, p. 263, ed. B. Lehnert, Cambridge.
Schmidt, H. U., 1968. *Structure and development of solar active regions*, p. 95, ed. K. O. Kiepenheuer, Reidel, Dordrecht.
Schröter, E. H., 1971. *Solar magnetic fields*, p. 167, ed. R. Howard, Reidel, Dordrecht.
Sheeley, N. R., 1969. *Sol. Phys.*, **9**, 347.
Sheeley, N. R., 1971. *Solar magnetic fields*, p. 310, ed. R. Howard, Reidel, Dordrecht.
Sheeley, N. R., 1972. *Sol. Phys.*, **25**, 98.
Sheeley, N. R. & Bhatnagar, A., 1971. *Sol. Phys.*, **19**, 338.
Simon, G. W. & Leighton, R. B., 1964. *Astrophys. J.*, **140**, 1120.
Simon, G. W. & Weiss, N. O., 1968. *Z. Astrophys.*, **69**, 435.
Simon, G. W. & Weiss, N. O., 1970. *Sol. Phys.*, **13**, 85.
Spitzer, L., 1956. *Physics of fully ionized gases*, Interscience, New York.
Vrabec, D., 1971. *Solar magnetic fields*, p. 329, ed. R. Howard, Reidel, Dordrecht.

Vrabec, D., 1974. *Fine structure of the chromosphere*, ed. R. G. Athay, Reidel, Dordrecht.
Weiss, N. O., 1964a. *Phil. Trans. A*, **256,** 99.
Weiss, N. O., 1964b. *Mon. Not. R. astr. Soc.*, **128,** 225.
Weiss, N. O., 1966. *Proc. R. Soc. A*, **293,** 310.
Weiss, N. O., 1969. *Plasma instabilities in astrophysics*, p. 153, eds D. G. Wentzel and D. E. Tidman, Gordon and Breach, New York.
Weiss, N. O., 1971. *Solar magnetic fields*, p. 757, ed. R. Howard, Reidel, Dordrecht.
Weiss, N. O., 1974. *Adv. Chem. Phys.*, to be published.
Wilson, P. R., 1968. *Sol. Phys.*, **3,** 243.
Wilson, P. R., 1972. *Sol. Phys.*, **27,** 363.
Wilson, P. R., 1973. *Sol. Phys.*, **32,** 435.
Wilson, P. R., 1974a. *Sol. Phys.*, **35,** 111.
Wilson, P. R., 1974b. *Sol. Phys.*, in press.
Yun, H. S., 1970. *Astrophys. J.*, **162,** 975.
Zwaan, C., 1968. *A. Rev. Astr. Astrophys.*, **6,** 135.